APPENDIX

Kittel[22] has pointed out that the methods employed in this article bear a resemblance to Chambers'[23] solution to the classical Boltzmann transport equation. Investigation of this point has revealed the following very simple derivation of the solutions to Bloch's equation for $T_1=T_2$. By accounting for all magnetization entering the cone at times previous to the time being considered, the rate of arrival of magnetization elements at an angle ϕ, where ϕ is measured only once around the cone, may be determined:

$$\text{Rate}=\sum_{n=0}^{\infty} M(T_1)^{-1}\exp[-(\phi+2\pi n)/(\Omega T_1)]$$
$$=M(T_1)^{-1}\exp[-(\phi/\Omega T_1)]/[1-\exp(-2\pi/\Omega T_1)].$$

But this must equal $M(\phi)\Omega$, the flow rate by the position, ϕ. Thus

$$M(\phi)=M(\Omega T_1)^{-1}\exp(-\phi/\Omega T_1)[1-\exp(-2\pi/\Omega T_1)]^{-1}.$$

This expression substituted into (5), (6), and (7) with a range of integration from 0 to 2π yields (11), (12), and (13). Note that as $\Omega T_1\rightarrow\infty$, $M(\phi)\rightarrow M/2\pi$, which explains the uniform distribution of magnetization in the cone at high radio frequency fields.

It may be possible to extend this approach to account for all magnetization scattered by various relaxation processes into each trajectory passing through a point on the reference sphere, and thus to obtain a completely general classical description of magnetic resonance.

[22] C. Kittel (private communication).
[23] R. G. Chambers, Proc. Phys. Soc. (London) **A65**, 458 (1952), see also V. Heine, Phys. Rev. **107**, 436 (1957).

PHYSICAL REVIEW VOLUME 125, NUMBER 4 FEBRUARY 15, 1962

De Haas-van Alphen Effect in Bismuth-Tellurium Alloys*†

DANIEL WEINER‡
Department of Physics and Institute for the Study of Metals, University of Chicago, Chicago, Illinois
(Received June 2, 1961)

De Haas-van Alphen measurements have been made on pure bismuth and several bismuth-tellurium alloys. It is found that the observed variation of external cross section and cyclotron effective mass with tellurium concentration and magnetic field orientation can be interpreted using a special case of Cohen's nonellipsoidal model of bismuth. The results indicate that there is a thermal energy gap between the conduction and valence band of about 0.046 ev in agreement with various optical experiments and that there are six electron "ellipsoids." The results also agree with a model for the hole band involving one light-hole ellipsoid and one heavy-hole ellipsoid and are used as evidence against some other possible models for the hole band.

I. INTRODUCTION

RECENT experiments[1] indicate that the Fermi surface of bismuth may not be parabolic-ellipsoidal, so that both the absolute and relative size of its effective mass components depend on the Fermi energy. The details of this dependence, if known, would establish many of the parameters in Cohen's[2] nonellipsoidal theory of the bismuth band structure.

The Fermi level in bismuth may be conveniently changed without appreciably affecting the crystal potential by addition of an electron donor such as tellurium. Each tellurium atom presumably contributes one electron to the Fermi sea. Since the instrinsic number of conduction electrons in bismuth is small (about 10^{-5}/atom), very little tellurium is needed to increase it appreciably.

A powerful method of studying the band structure of these alloys is provided by the de Haas-van Alphen effect.[3] It measures the extreme cross-sectional areas of the Fermi surface and their energy derivative. Furthermore, the interpretation of the effect is unaffected by the changes in collision times on alloying. Also, as we shall see later, we can find the number of equivalent ellipsoid-like pieces of the electron Fermi surface with our de Haas-van Alphen data and a knowledge of the amount of tellurium present in those alloys in which we have filled the hole band. In alloys where we have not filled the hole band, a knowledge of the tellurium concentration helps give us an average density of states.

Indeed, Shoenberg and Uddin[4] have already explored

* Submitted as a thesis in partial fulfillment of the requirements for the degree of doctor of philosophy at the University of Chicago.
† This work was supported in part by a grant from the National Science Foundation to the University of Chicago for research on the solid state properties of bismuth, antimony, and arsenic.
‡ Now at Hughes Research Laboratories, Malibu, California.
[1] B. Lax, Bull. Am. Phys. Soc. **5**, 167 (1960).
[2] M. H. Cohen, Phys. Rev. **121**, 387 (1961).
[3] D. Shoenberg, *Progress in Low-Temperature Physics*, edited by C. J. Gorter (Interscience Publishers, Inc., New York, 1957), Vol. 2, Chap. 8.
[4] D. Shoenberg and M. Z. Uddin, Proc. Roy. Soc. (London) **A156**, 701 (1936).

TABLE I. Atomic percent tellurium in bismuth and the alloys.

Sample and sample weight	Calculated atomic percent	Analyzed atomic percent		Ratio of Te in sample to Te in sample No. 4		Best estimate of composition (atomic %)
		Left of sample	Right of sample	Calculated	Analyzed	
No. 1, 0.36g	1.1×10^{-3}	2.1×10^{-3}	2.1×10^{-3}	0.10	0.15	$(2.1\pm0.5)\times10^{-3}$
No. 2, 0.62g	2.9×10^{-3}	3.7×10^{-3}	3.9×10^{-3}	0.27	0.28	$(3.8\pm0.5)\times10^{-3}$
No. 3, 0.63g	4.0×10^{-3}	4.2×10^{-3}	6.8×10^{-3}	0.38	0.41	$(5.5\pm1.5)\times10^{-3}$
No. 4, 0.75g	10.8×10^{-3}	13.0×10^{-3}	13.8×10^{-3}	1.00	1.00	$(13.4\pm0.7)\times10^{-3}$
Bismuth, 0.32g	0	0		0	0	0

the de Haas-van Alphen effect in a number of dilute bismuth alloys. However, their work was admittedly exploratory and was done at only one temperature and two magnetic field orientations for each alloy which is insufficient to provide the necessary information. Furthermore, subsequent to these experiments the techniques of preparing and analyzing pure, uniform, single-crystal samples have been considerably improved. Hence, a more thorough study of these alloys appears worthwhile.

II. EXPERIMENTAL METHODS

A. Sample Preparation and Analysis

Bismuth of suitable purity was prepared by drip melting 99.998% label purity Cerro de Pasco bismuth into a quartz boat and zone-refining it for 20 passes under a vacuum of 10^{-4} mm Hg using a 450-kc/sec inductive heater. An essentially identical procedure by Barrett[5] yielded bismuth with a residual resistance ratio of $R_{300}/R_{1.5}=1180$ which exceeds the best in the literature to date. A spectrographic analysis of some of the alloyed bismuth showed a negligible impurity level. This will be discussed in detail later. The resulting bar of bismuth was cut with a jeweler's saw into 100-gram pieces and then etched; the end pieces were discarded.

An alloy containing 0.2 weight percent tellurium was prepared by melting 100 g of pure bismuth with 0.15 g of purified Fisher tellurium that had been cleaved from the interior of a rod to prevent oxide contamination. The resulting ingot was zone leveled for 6 passes in a quartz boat under a vacuum of 10^{-4} mm Hg. Then, before each sample was prepared, a suitably sized piece was cleaved with a steel scalpel from the interior of this alloy. This piece along with a freshly etched and polished 100-g piece of pure bismuth was put into a quartz boat which had been etched for a few hours in HF to remove irregularities that might nucleate grains. These were melted together and the resulting bar was zone leveled for 6 passes under a 10^{-4}-mm Hg vacuum. It was found, however, that the HF etch did not insure the production of single crystals of a useable size. In preparing later samples, the interior of the boat was therefore covered with a thick coat of carbon from an acetylene flame before the last zone-melting pass. This procedure always resulted in a single-crystal sample for almost the entire length of the boat.

A small piece was cut from the central portion of each sample with a jeweler's saw and was easily cleaved along the trigonal plane with a steel scalpel after being cooled in liquid nitrogen. Its crystallographic directions were determined with the aid of the principal cleavage plane and a Laue pattern. The sample was cut perpendicular to a binary axis with a toothless band saw using 600-mesh carborundum suspended in water. This cut and the cleavage plane were used to orient the sample on the sample holder by aligning it with the suspension rod with a straight edge. Laue patterns of samples attached to the sample holder showed typical errors in alignment of $\sim1°-2°$.

The composition of the alloys was determined by Miss M. Bachelder of this Institute by a procedure devised by Wiberley *et al.*[6] Ten grams of material were taken from that part of each bar adjacent to either side of the sample. Each 10-g piece was dissolved in HNO_3, concentrated by evaporation in a steam bath, and diluted in HCl. The tellurium was precipitated out with $SnCl_2$, and, after standing, the precipitate was filtered out, washed and dried. The filtrate was dissolved in hot H_2SO_4, cooled and diluted to a specified volume with more H_2SO_4. The absorbance of these solutions was measured with a Beckman Model D spectrophotometer at 5200 A. From the absorbance one can determine the tellurium concentration by comparison with calibration curves made using synthetic samples. The scatter in these calibration curves from a straight line going through the origin indicates an error of about ±0.0005 atomic percent for our tellurium analysis.

Information relating to the amount of tellurium in the samples is in Table I. We note that calculated concentration is usually above 20% lower than the concentration given by analysis procedure described above. This situation is not implausible because the small region of the 0.4 atomic percent alloy with which the final alloys were doped may well have had a 20% higher concentration than the mean. The final estimates of the tellurium concentration are the means of the

[5] C. S. Barrett (private communication).

[6] S. E. Wiberley, L. G. Bassett, A. M. Burrill and H. Lyng, Anal. Chem. **25**, 1586 (1953).

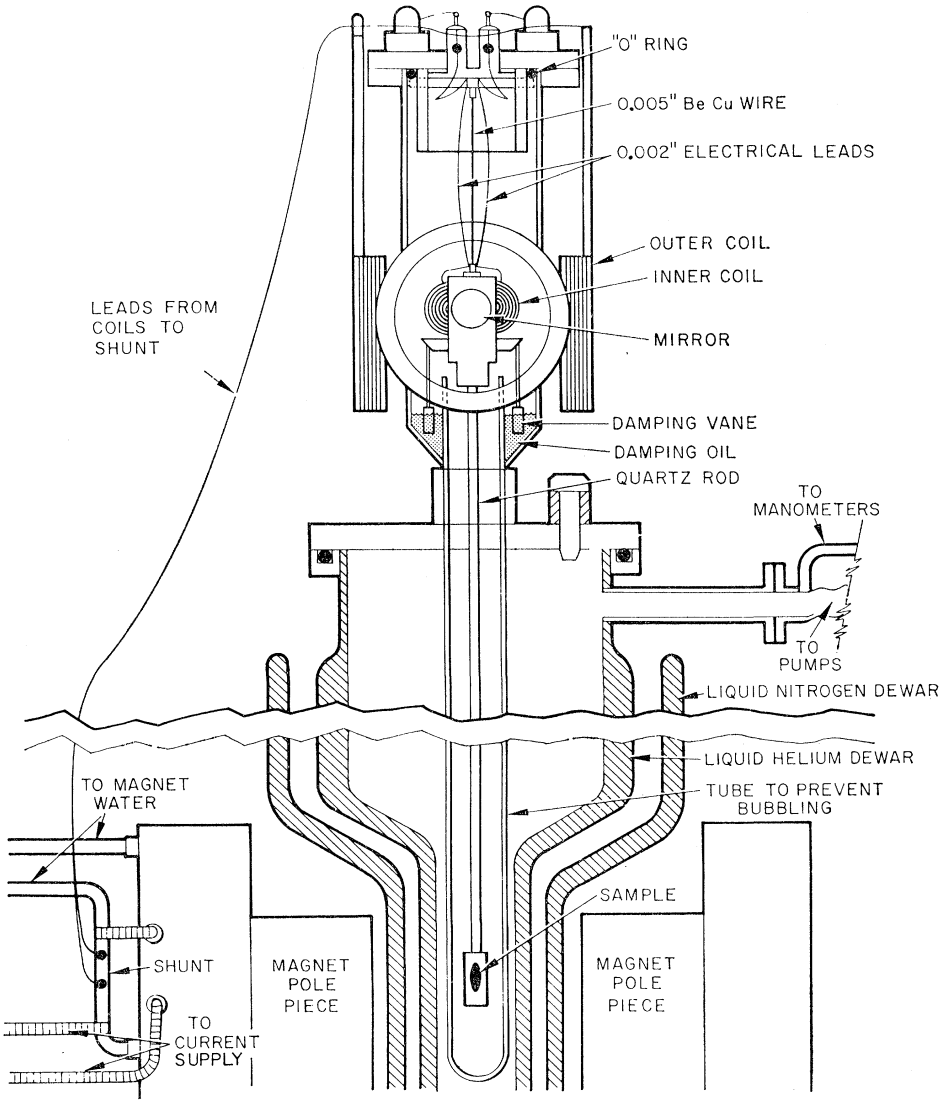

FIG. 1. Schematic drawing of the apparatus.

values for the analysis of material on either side of the sample. The error given comes from two sources. One is the error estimated from the scatter in the calibration curve of ± 0.0005 atomic percent. The other is just half the difference of the analysis values for the material on either side of the sample.

Spectroscopic analysis of the 0.4 atomic percent and the No. 3 alloys show the presence of Ag and Cu impurities only and these with a concentration of ~ 0.0001 weight percent. It has been our experience at this laboratory that these are the most difficult to remove by zone-refining so that other impurities should be at a much smaller level. Now Goetz and Focke[7] show that Ag and Cu are not electron donors or acceptors in bismuth. Hence the amount of relevant impurities appears small compared with the intrinsic carrier concentration of ~ 0.002 atomic percent.

[7] A. Goetz and A. B. Focke, Phys. Rev. **45**, 185 (1934).

B. Cryogenics and Magnet

The cryogenics consists of standard concentric nitrogen and helium Dewars that neck down to a $2\frac{1}{8}$-in. o.d. in the vicinity of the pole caps. There are provisions for pumping down to about 1.2°K. The pressure of the liquid helium in the helium dewar is measured by means of oil and mercury manometers and a cathetometer. The sample is immersed directly in liquid helium. Above the λ point, the disturbing effect arising from bubbling at the liquid helium surface was suppressed by surrounding the sample holder with a long closed tube having small holes both above and below the liquid helium surface.

The magnet is a standard low voltage electromagnet with 4 in. cylindrical pole caps, a $2\frac{3}{8}$-in. pole gap and a rotatable base. In this experiment it was used to produce fields up to 6000 gauss that were uniform to about 0.1% over the samples. The current through

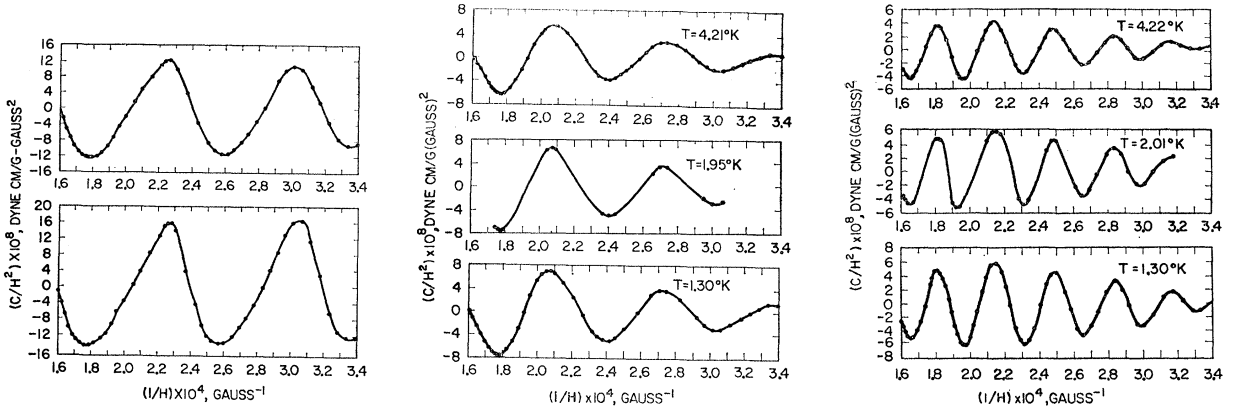

FIG. 2. C/H^2 versus $1/H$ for the magnetic field 78° from the trigonal axis with the binary axis vertical, (a) in pure bismuth, (b) in alloy No. 1, (c) in alloy No. 3.

the magnet coil was electronically controlled via the field windings of the current generator to about 0.1%. The field-current relationship was determined to $\pm\frac{1}{2}\%$ with a flip coil that had been calibrated by nuclear magnetic resonance. During the experiment, the current could be read to about $\pm 0.2\%$.

C. Susceptibility Measurement Assembly

De Haas-van Alphen oscillations in the susceptibility were measured by the standard method of determining the torque exerted on an anisotropic crystal when a homogeneous magnetic field is applied along a direction not collinear with a principal crystallographic axis of the crystal.[8] The main features of the apparatus as shown in Fig. 1 are as follows: The samples are glued to a small quartz plate with a cleavage plane flush against the plate. The plate is fused to a long quartz rod attached to an assembly supporting a mirror, damping vanes and a coil of about 100 turns of No. 30 copper wire. This whole assembly is suspended by a 3-inch piece of 0.005-in. diameter BeCu wire having a torque constant of 100 dyne cm/radian so that the damping vanes extend into an oil cup and the sample is centered between the poles of the magnet. The torque on the sample is determined by reading an illuminated scale $4\frac{1}{2}$ meters away from the apparatus through the mirror with a telescope. The scale can be read to about 0.3 mm.

In the alloys, the steady susceptibility is often much greater than the oscillating de Haas-van Alphen component for our available magnetic fields. With our low torque constant suspension, this can cause serious changes in sample orientation with magnetic field. Also small fluctuations in the magnet current ($\sim 0.1\%$) cause changes in the steady torque are comparable in size to the de Haas-van Alphen oscillations. Hence we use a simple but effective scheme to buck out the steady susceptibility, a scheme that does not use the feedback mechanisms of previous methods.[3]

[8] D. Shoenberg, Proc. Roy. Soc. (London) **A170**, 341 (1939).

Magnet current taken from a water cooled shunt was used to activate three parallel coils. One of these, the 5-ohm coil that is mounted on the suspended assembly (Fig. 1) is connected to the outside by two loose 0.002-in copper wires. The other two coils, of ~ 0.1 ohm each, are mounted outside with their plane perpendicular to the plane of the 5-ohm coil. The torque exerted on the 5-ohm coil by the other coils is proportional to the product of the current in each coil and hence to the square of the magnet current. In the region where the magnetic field is proportional to the magnet current, the torque is proportional to the square of the field. Since the torque due to the steady susceptibility is also proportional to the square of the field, we can in principal adjust our shunt such that these two torques cancel for all values of the field. In practice, magnet nonlinearity and the fields of the earth and the magnet at the coil make the bucking incomplete. However, for magnetic fields of interest, the cancellation was 98% effective and allowed observations of the de Haas-van Alphen oscillations only about 1/500 as large as the steady susceptibility at 1.3°K.

Distortions of the oscillations due to nonlinearity in the bucking scheme are small and may be easily corrected in the following manner. We measure the torque for a given arrangement at an elevated temperature where there are no oscillations, subtract this curve from the curve with oscillations and divide by H^2. The resulting curve should differ from the true curve by only a constant due to the change of steady susceptibility with temperature.

III. RESULTS

Some examples of the results are shown in Fig. 2. These are more satisfactory than most results for the following reasons. The field orientation is such that there is a contribution to the couple from only one extremal cross-sectional area so that there are no

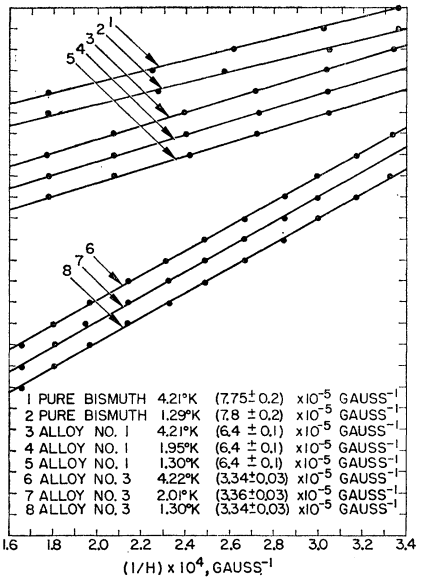

FIG. 3. Values of $1/H$ for the maxima and minima of C/H^2 in the curves of Fig. 2 versus successive half integers.

beats.[9] Also, the damping is relatively small because the cyclotron mass is small. Finally, the amplitude is large because of the small mass and because the field is not too close to a principal axis. These curves were derived from the experimental measurements as described in Sec. II.

The theoretical expression for the couple per unit mass[3,9] is as follows:

$$\frac{C}{H^2}=-\frac{A}{\rho}\sum_{i=1}^{3}\frac{a_i}{T^{\frac{1}{2}}}\left(\frac{2\pi^2kT}{\beta_iH}\right)^{\frac{3}{2}}\sum_{p=1}^{\infty}(-1)^p \times\frac{\sin\left(\frac{2\pi pE_0}{\beta_iH}-\frac{\pi}{4}\right)\exp(-2\pi^2pkx_i/\beta_iH)}{2p^{\frac{1}{2}}\sinh(2\pi^2pkT/\beta_iH)}. \quad (1)$$

Here, the quantities of interest to us are C, the couple per unit mass; H, the magnetic field; $\beta_i=ehc^{-1}(d\mathcal{A}/dE)_i^{-1}$, the effective double Bohr magneton for "ellipsoid" i; $E_0=\beta_ie^{-1}h^{-1}c\mathcal{A}_i$, where $\mathcal{A}_i$ is the extremal cross section of the Fermi surface "ellipsoid" i perpendicular to the field; T, the absolute temperature; and x_i, an effective temperature due to scattering of electrons. In Eq. (1), k, e, h, and c have their usual meanings.

For our purposes, we need only consider the $p=1$ term. The effect of the harmonics on the deduction of the correct values of β/E_0 and β from our curves is very small even in the worst case, that of pure bismuth with the magnetic field nearly perpendicular to the trigonal axis.[9] For other field directions and for other materials, the larger masses and higher effective temperatures x_i suppress the harmonics much further.

[9] J. S. Dhillon and D. Shoenberg, Phil. Trans. Roy. Soc. (London) A248, 1 (1955).

According to Eq. (1), if we plot $1/H$ for successive maximima and minima of CH^{-2} vs $1/H$ we should get straight lines of slope β/E_0. Examples of such plots corresponding to the curves of Fig. 2 are shown in Fig. 3.

The deviations of these points from straight lines are caused by many factors. At high fields, effects due to harmonics and changes of sample orientation with respect to the field caused by the torque are apparent. These errors tend to displace the maxima to one side and the minima to the other side of their true positions. At lower fields and in the more concentrated alloys, the small amplitude leads to difficulty in locating the maxima and minima. In general, the errors are not cumulative and are such that they define a slope to within about $\pm 2\%$. This is comparable to the error expected from misorientation of the sample.

The effect of beats between different pockets of the Fermi surface is seldom of any consequence in our experiments. Usually, one periodic term dominates CH^{-2}. In some cases, where the contribution to CH^{-2} comes from very similar portions of the Fermi surface a small modulation of both the amplitude and the period of CH^{-2} appears but again the errors are not cumulative. Occasionally, a portion of a curve is greatly distorted by beats and CH^{-2} is definitely not periodic in $1/H$. These data are ignored.

The temperature dependence of C for a given $\mathbf{H}$ determines β. The ratio of the amplitude of the de Haas-van Alphen oscillations at temperature T_1 and T_2 for a given field H is, neglecting harmonics

$$\frac{C_1}{C_2}=\frac{T_1\sinh(2\pi^2kT_2/\beta H)}{T_2\sinh(2\pi^2kT_1/\beta H)}\equiv\frac{\sinh\mu s}{\mu\sinh s}, \quad (2)$$

where $\mu=T_2/T_1$, $s\equiv 2\pi^2kT_1/\beta H$. Plots of C_1/C_2 vs s are made for each μ considered. From these plots and from the experimental values of C_1/C_2 for several values

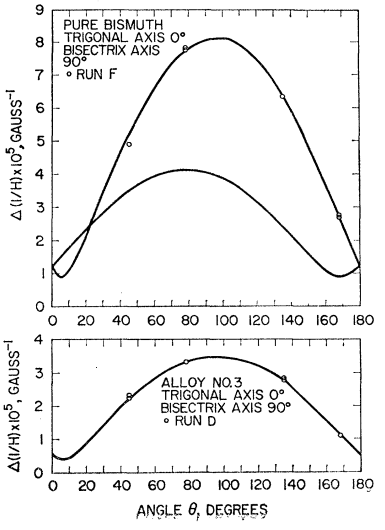

FIG. 4. Angular dependence of the period for pure bismuth and alloy No. 3 with the binary axis vertical. The solid lines are the theoretical curves.

of H, the corresponding values of s are found. Then $\beta=2\pi^2kT_1/sH$ is computed for each value of H. The spread from the mean value of β is usually attributable to uncertainty in the amplitude measurements except at high fields where bucking errors may become important.

The experimental results for β/E_0 are shown in Figs. 4–6, for the variety of experimental conditions for which it was determined. The error in estimating the slope β/E_0 is about 0.1×10^{-5} gauss^{-1} which is consistent with the observed scatter except when we expect beats. In the latter case the scatter is about twice this size. The solid lines in the plots for pure bismuth are the results of calculating β/E_0 from the ellipsoidal-parabolic model of the Fermi surface for conduction electrons in bismuth,[3] using the relation

$$2m_0E_0=\alpha_1p_x^2+\alpha_2p_y^2+\alpha_3p_z^2+2\alpha_4p_yp_z, \qquad (3)$$

with $\alpha_1=202$, $\alpha_2=1.67$, $\alpha_3=70$, $\alpha_4=7.0$, and $E_0=0.0177$ ev. Our values of α_3 and α_4 give a slightly better fit to our data than those of Aubrey[10] ($\alpha_3=83.3$, $\alpha_4=8.33$). The difference may arise from a systematic error in aligning our sample but, as it is our purpose to compare the relative change in β/E_0 upon alloying, this effect is unimportant. In any case, the disagreement is small and the effect on the volume of the Fermi surface is negligible. The solid lines in the case of the alloys represent a scaling down of the calculated β/E_0 in bismuth (for the relevant ellipsoids only) by the factor indicated in Table V. We note that deviations from the theoretical curves are greatest where we expect beats. Hence, we see that to a good approximation for the angles measured, the primary effect of alloying is to change only the size of the Fermi surface and not its shape or tilt.

The results derived from the temperature dependence of the amplitude are shown in the last two columns of Table II. Here β_0 is true double Bohr magneton so β/β_0 is the ratio of the true electron mass to the relevant cyclotron effective mass. We note that there is a general increase in effective mass for a given orientation upon alloying. The quantity would represent the Fermi temperature T_F in an ellipsoidal-parabolic model of the Fermi surface. We note that to within experimental error, T_F is independent of angle and the temperatures used in its determination.

There is no data for sample No. 4 and the data for sample No. 2 is poor because of the large collision damping effects. The largest damping in No. 4 is to be expected as it contains the most scatterers. The damping in No. 2 is greater than in No. 3 probably due to some mistreatment during cutting.

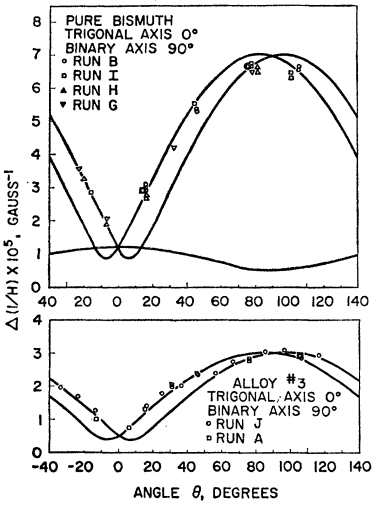

FIG. 5. Angular dependence of the period for pure bismuth and alloy No. 3 with the bisectrix axis vertical. The solid lines are the theoretical curves.

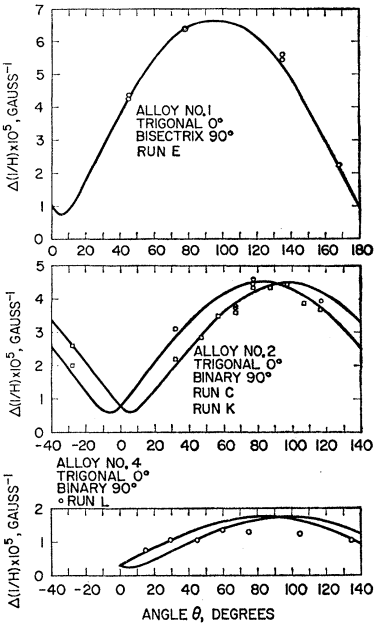

FIG. 6. Angular dependence of the period for alloy No. 1 with the binary axis vertical and for alloys No. 2 and No. 4 with the bisectrix axis vertical. The solid lines are the theoretical curves.

IV. CONCLUSIONS

The conclusions are treated in four separate subsections: (A) the energy gap in bismuth, (B) comparison of the angular dependence with the non-ellipsoidal model, (C) number of "ellipsoids", and (D) density of states in bismuth.

A. The Energy Gap in Bismuth

Table III shows a summary of the de Haas-van Alphen effect data in several substances for a particular direction of the field with respect to the crystal lattice. Because $\mathcal{A}k^{-1}(d\mathcal{A}/dE)^{-1}$ is approximately independent of angle for a given substance, and because the shape of the Fermi surface is approximately unchanged by doping, the values of the ratios $\mathcal{A}/\mathcal{A}_{Bi}$, $(d\mathcal{A}/dE)/(d\mathcal{A}/dE)_{Bi}$, and $\mathcal{A}/k(d\mathcal{A}/dE)/[\mathcal{A}/k(d\mathcal{A}/dE)]_{Bi}$ for the various substances as shown in Table III are represent-

[10] J. E. Aubrey, thesis, Cambridge University, 1959 (unpublished).

TABLE II. Values of $\mathfrak{A}/k(d\mathfrak{A}/dE)$ and β for bismuth and the alloys.

Sample	Run	Temperature (°K) High	Low	Sample orientation[a]	Angle of field from trigonal	$\Delta(1/H)=\beta/E_0=eh/c\mathfrak{A}$ (10^{-5} gauss^{-1})	$\mathfrak{A}/k(d\mathfrak{A}/dE)$ (°K)	$\beta/\beta_0=(d\mathfrak{A}/dE)/2\pi m_0$
Alloy No. 3	*D*	4.22	1.30	2	78°	3.34	325±7	81 ±2
	D	4.22	2.10	2	78°	3.34	322±7	80 ±2
	D	4.22	1.30	2	45°	2.28	309±4	52.5±1.0
	D	4.22	1.30	2	135°	2.80	309±8	64.5±2.0
	A	4.23	1.29	1	76°	2.80	316±10	66 ±2
	A	4.23	1.29	1	106°	2.91	292±10	63 ±2
Alloy No. 2	*C*	4.21	1.33	1	77°	4.5	~250	~82
	C	4.21	1.99	1	77°	4.5	~250	~82
	C	4.21	1.33	1	117°	3.75	~270	~75
Alloy No. 1	*E*	4.21	1.30	2	45°	4.3	226±10	72 ±3
	E	4.21	1.30	2	78°	6.4	228±15	108 ±7
	E	4.21	1.95	2	78°	6.4	218±8	104 ±4
	E	4.21	1.30	2	135°	5.5	216±5	88.5±2.0
Bismuth	*F*	4.21	1.29	2	78°	7.8	195±7	113 ±4
	F	4.21	1.98	2	168°	2.75	196±7	40.0±1.5
	F	4.21	1.29	2	168°	2.75	193±7	39.5±1.5
	B	4.21	1.21	1	16½°	3.00	203±5	45.5±1.0
	B	4.21	1.99	1	16½°	3.00	201±5	45 ±1
	B	4.21	1.21	1	46½°	5.33	200±8	79 ±4
	B	4.21	1.21	1	76½°	6.67	195±7	97 ±3
	B	4.21	1.21	1	106½°	6.56	~205	~100

[a] 1 means bisectrix vertical; 2 means binary vertical.

ative of those for any angle. Here we see a marked increase in effective mass with Fermi level.

The particular choice of field direction to be used in this calculation was made for the following reasons: Experimentally, beats are absent and the amplitude of the susceptibility oscillations is relatively large; theoretically, the pertinent cross-sectional area of the Fermi surface is only 5% greater than the minimum possible cross-sectional area, i.e., that for which the field is along axis 2. In this direction certain expressions in Cohen's[2] non-ellipsoidal-nonparabolic model of the bismuth band structure have a particularly simple from.

The cross-sectional area of the Fermi surface cut by a plane perpendicular to the 2 axis at p_2 is, in Cohen's notation,

$$\mathfrak{A}=\frac{2\pi(m_1m_3)^{\frac{1}{2}}}{E_g}\left(E-\frac{p_2^2}{2m_2}\right)\left[\left(E-\frac{p_2^2}{2m_2}\right)(1+\beta_1+\beta_3)+E_g-A_2p_2+\frac{p_2^2}{2m_2}+\frac{p_2^2}{2m_2'}\right]. \quad (4)$$

Now we make the simplifying assumption that A_2 is small so that we may take $p_2=0$ for the extremal cross section and that if H is off axis 2 we may still use Eq. (4) if we substitute the appropriate cyclotron mass for $(m_1m_3)^{\frac{1}{2}}$. We will see in Sec. *B* that these assumptions lead to agreement with experiment for the angular dependence of $\mathfrak{A}$. Then using Eq. (4) and the information in Table III we can derive values for $E_g/(1+\beta_1+\beta_3)$, $(m_1m_3)^{\frac{1}{2}}$ and E in the following manner.

Let $\lambda\equiv1+\beta_1+\beta_3$. Then, with the above assumptions, we have

$$\mathfrak{A}=2\pi(m_1m_3)^{\frac{1}{2}}E(1+\lambda E/E_g), \quad (5)$$

and

$$d\mathfrak{A}/dE=2\pi(m_1m_3)^{\frac{1}{2}}(1+2\lambda E/E_g). \quad (6)$$

Accordingly, the ratio for two different values of E is

$$\frac{\mathfrak{A}_2}{\mathfrak{A}_1}=\frac{\lambda E_2}{E_g}\left(1+\frac{\lambda E_2}{E_g}\right)\Big/\frac{\lambda E_1}{E_g}\left(1+\frac{\lambda E_1}{E_g}\right),$$

$$\left(\frac{d\mathfrak{A}}{dE}\right)_2\Big/\left(\frac{d\mathfrak{A}}{dE}\right)_1=\left(1+2\frac{\lambda E_2}{E_g}\right)\Big/\left(1+2\frac{\lambda E_1}{E_g}\right),$$

TABLE III. Summary of results for the magnetic field 78° from the trigonal axis with the binary axis vertical.

Substance	β/E_0 (10^{-5} gauss^{-1})	$\mathfrak{A}/k(d\mathfrak{A}/dE)$ (°K)	β/β_0	$\mathfrak{A}/\mathfrak{A}_{Bi}$	$(d\mathfrak{A}/dE)/(d\mathfrak{A}/dE)_{Bi}$	$\frac{\mathfrak{A}/k(d\mathfrak{A}/dE)}{\mathfrak{A}/k(d\mathfrak{A}/dE)_{Bi}}$	$\lambda E/E_g$		E(ev)	T(°K)	E_g/λ (ev)
Bismuth	7.80±0.05	195±7	113±4	1.00	1.00	1.00	0.50	0.48	0.022	260	0.046
Alloy No. 1	6.40±0.05	221±8	105±4	1.22±0.01	1.08±0.05	1.13±0.05	0.58	0.56	0.026	300	0.045
Alloy No. 3	3.34±0.05	323±7	80½±2	2.34±0.05	1.41±0.05	1.66±0.05	0.88	0.88	0.041	475	0.046

from which it follows that

$$\lambda\frac{E_1}{E_g}=\frac{1}{2}\left\{\left[\left(\frac{\mathfrak{A}_2}{\mathfrak{A}_1}-1\right)\Big/\left(\frac{\mathfrak{A}_2}{\mathfrak{A}_1}-\frac{(d\mathfrak{A}/dE)_2^2}{(d\mathfrak{A}/dE)_1^2}\right)\right]^{\frac{1}{2}}-1\right\}, \quad (7)$$

and

$$\lambda\frac{E_2}{E_g}=\frac{1}{2}\left[\left(1+2\lambda\frac{E_1}{E_g}\right)\frac{(d\mathfrak{A}/dE)_2}{(d\mathfrak{A}/dE)_1}-1\right]. \quad (8)$$

Dividing Eq. (5) by Eq. (6), we find that Fermi energy E_1 is given by

$$E_1=\frac{\mathfrak{A}_1}{(d\mathfrak{A}/dE)_1}\left[\frac{1+2\lambda E_1/E_g}{1+\lambda E_1/E_g}\right]. \quad (9)$$

Dividing Eq. (9) by Eq. (7) yields an expression for E_g/λ. Finally the cyclotron mass at the bottom of the band is given, according to Eq. (6), by

$$(m_1m_3)^{\frac{1}{2}}=\frac{1}{2\pi}\left(\frac{d\mathfrak{A}}{dE}\right)_1\left(1+2\lambda\frac{E_1}{E_g}\right)^{-1}. \quad (10)$$

Note that in evaluating Eqs. (8)–(10) we must use Eq. (7).

The results of such a calculation are shown in Table III. From the data for any pair of substances we can calculate a value of $\lambda E/E_g$ for each member. The values of $\lambda E/E_g$ calculated for the three possible pairs of substances listed in the table are seen to be consistent. The value of the Fermi energy in bismuth of 0.022 ev is in excellent agreement with the value obtained by Wolff[11] of 0.022 ev. Our value of E_g/λ, which represents the thermal energy gap if $A_2=0$ is 0.046 ev. Now Wolff[11] derives an energy gap of 0.42 ev by assuming that an indirect transition from the top of the valence band to Fermi surface in the conduction band as is shown in Fig. 7(a) is responsible for optical absorption. Since the transition is indirect the same treatment holds if one band is not on top of the other as is shown in Fig. 7(b). Similarly, Brown *et al.*[12] obtain a gap of 0.047 ± 0.003 ev from magneto-optical experiments assuming the valence band is just below the conduction band. However, they point out that if the bands are displaced by a small amount in k space their result should be essentially unchanged. So we may interpret both of these gaps as thermal gaps. Hence our gap is in good agreement with those obtained from optical measurements. However, it should be noted that this very close agreement is somewhat fortuitous as even in the most favorable case, our error is such that $\lambda E/E_g$ may be anywhere between 0.3 and 0.7 which corresponds to values of E between 0.021 ev and 0.024 ev and of E_g/λ between 0.035 ev and 0.070 ev. Nevertheless, the results suggest that the specific model of Jain[13] with a thermal gap of 0.007 ev between the conduction and valence band is incorrect.

[11] P. A. Wolff (to be published).
[12] R. N. Brown, J. G. Mavroides, M. S. Dresselhaus and B. Lax, *The Fermi Surface*, edited by W. A. Harrison and M. B. Webb (John Wiley & Sons, Inc., New York, 1960), pp. 203–209.
[13] A. L. Jain, Phys. Rev. **114**, 1518 (1959).

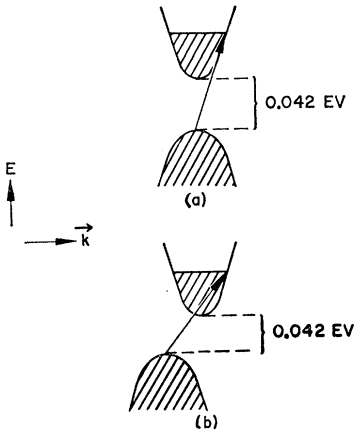

FIG. 7. Optical absorption of radiation in bismuth by an indirect transition, (a) when the hole and electron band extrema are at the same point in k space, (b) when these extrema are somewhat removed from each other in k space.

Finally we note that the cyclotron mass at the bottom of the band is about half the cyclotron mass at the Fermi energy for pure bismuth.

B. Comparison of the Angular Dependence with the Non-Ellipsoidal Model

As we noted in Sec. II, $\mathfrak{A}k^{-1}(d\mathfrak{A}/dE)^{-1}$ is independent of angle; the $\mathfrak{A}$'s fit an ellipsoidal model for any substance and scale down by the same ratio for any given angle between various substances; and the cyclotron mass for a given angle depends on the Fermi level. Hence, the behavior of bismuth appears ellipsoidal-nonparabolic to within experimental error for the angles investigated. To show that this behavior is also consistent with Cohen's[2] model for the sizable values of E/E_g encountered in bismuth and its alloys, we will examine some pertinent special cases of his theory by suitable approximation methods in the following paragraphs.

The general form of the Fermi surface in Cohen's notation is

$$\left[p_1+A_1m_1\left(\frac{E}{E_g}-\frac{p_2^2}{2m_2E_g}\right)\right]^2\Big/2m_1E_g + \left[p_3+A_3m_3\left(\frac{E}{E_g}-\frac{p_2^2}{2m_2E_g}\right)\right]^2\Big/2m_3E_g = \left(\frac{E}{E_g}-\frac{p_2^2}{2m_2E_g}\right)\left[\left(\frac{E}{E_g}-\frac{p_2^2}{2m_2E_g}\right)(\beta_1+\beta_2)+1 + \frac{E}{E_g}-\frac{A_2p_2}{E_g}+\frac{p_2^2}{2m_2'E_g}\right]. \quad (11)$$

Now if we let $A_1=A_2=A_3=\beta_1=\beta_3=0$ and $m_2=m_2'$, we have

$$\frac{p_1^2}{2m_1E_g}+\frac{p_3^2}{2m_3E_g}=\left(\frac{E}{E_g}-\frac{p_2^2}{2m_2E_g}\right)\left(\frac{E}{E_g}+1+\frac{p_2^2}{2m_2E_g}\right) =\frac{E}{E_g}\left(\frac{E}{E_g}+1\right)-\frac{p_2^2}{2m_2E_g}-\left(\frac{p_2^2}{2m_2E_g}\right)^2. \quad (12)$$

This special case is of interest for the following reasons: first, if $m_2=m_2'$, this formula holds exactly if there are three "ellipsoids."[2] Now the best evidence to date, the new interband magnetoreflection experiments by Brown *et al.*,[12] suggest that under the assumption of a three-"ellipsoid" model m_2 and m_2' do not differ by more than 20%.[2] Also we know that there are either three or six "ellipsoids."[2] Hence, if all our experiments are consistent with the three-"ellipsoid" models there must be three "ellipsoids." Otherwise there are six. Second, suppose that we find that there are six "ellipsoids." This means[2] that either A_1, $\beta_1\neq 0$ or A_2, A_3, $\beta_2\neq 0$. Now if the angular dependence computed for $A_i=\beta_i=0$ fits our experiments, we will have shown that Cohen's theory is capable of explaining the angular dependence of the de Haas-van Alphen effect, and we will have suggested that the A_i's and β_i's that do not vanish by symmetry are nevertheless small.

Now we note that if $p_2^2/2m_2E_g\ll 1$ so that we can neglect its square, Eq. (12) reduces to an ellipsoidal-nonparabolic form,[1] i.e.,

$$p_1^2/2m_1E_g+p_2^2/2m_2E_g+p_3^2/2m_3E_g=\frac{E}{E_g}\left(\frac{E}{E_g}+1\right). \quad (13)$$

But since $m_2\gg m_1$, m_3 in bismuth, this should hold well except for points on the surface within a small cone of directions about axis 2. We will now demonstrate this explicitly.

The equation for the area of intersection of the surface described by Eq. (12) with a plane through axis 3 that makes an angle θ_0 with axis 2 as shown in Fig. 8 is

$$\mathfrak{A}=\frac{8}{3}\frac{E\left(\frac{E}{E_g}+1\right)}{\cos\theta_0}\frac{(m_2m_3)^{\frac{1}{2}}(\tau^2+\tau)^{\frac{1}{2}}}{\left\{\left[\nu^2+\frac{E}{E_g}\left(\frac{E}{E_g}+1\right)\right]^{\frac{1}{2}}+\nu\right\}^{\frac{1}{2}}}$$
$$\times\left\{\mathcal{K}[(1+\tau)^{-\frac{1}{2}}]-\left(1-\frac{1}{\tau}\right)\mathcal{E}[(1+\tau)^{-\frac{1}{2}}]\right\}, \quad (14)$$

where

$$\nu=\frac{1}{2}\left(\frac{m_2}{m_1}\tan^2\theta_0+1\right),$$

$$\tau=\left[\nu^2+\frac{E}{E_g}\left(\frac{E}{E_g}+1\right)\right]^{\frac{1}{2}}+\nu\Big/\left[\nu^2+\frac{E}{E_g}\left(\frac{E}{E_g}+1\right)\right]^{\frac{1}{2}}-\nu,$$

and

$$\mathcal{K}[p]=\int_0^{\pi/2}dx(1-p^2\sin^2x)^{-\frac{1}{2}},$$

$$\mathcal{E}[p]=\int_0^{\pi/2}dx(1-p^2\sin^2x)^{\frac{1}{2}}$$

are complete elliptical integrals of the first and second kinds. For Eq. (13) the corresponding equation is simply

$$\mathfrak{A}=2\pi\frac{E\left(\frac{E}{E_g}+1\right)}{\cos\theta_0}\frac{(m_2m_3)^{\frac{1}{2}}}{\left(\frac{m_2}{m_1}\tan^2\theta_0+1\right)^{\frac{1}{2}}}.$$

The results of evaluation of these formulas for various angles for the case $E/E_g=1$, $m_2/m_1=100$ which corresponds to alloy No. 3, are shown in Table IV. Even in this extreme case, the difference between the two areas is less than 1% for $\theta_0=15°$ which is very nearly the smallest experimental value of θ_0. Hence the angular dependence of Cohen's model and the ellipsoidal model should be the same for our experimental conditions.

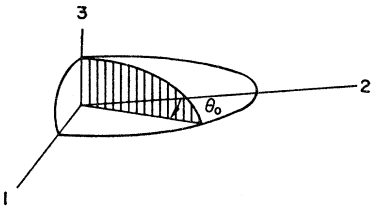

FIG. 8. Diagram showing the cross section of the nonellipsoidal Fermi surface that is tabulated in Table IV.

With the torque method, the amplitude of the de Haas-van Alphen oscillations disappears for the extremal cross sections corresponding to $\theta_0=0$ and for θ_0 near zero they are masked by oscillations from other pockets of the Fermi surface corresponding to larger θ_0 and smaller cyclotron mass. However, we may infer the size of cross sections for $\theta_0=0$ which we will need in Sec. C by applying Cohen's theory to our and other experiments. For our purposes, as noted before, it will be sufficient to look at the case of $A_i=\beta_i=0$.

Then for this special case, we have for $\mathfrak{A}(\theta_0)$ and $\mathfrak{A}/d\mathfrak{A}/dE(\theta_0)$ for the ellipsoidal (subscript e) and nonellipsoidal (subscript n) cases:

$$\mathfrak{A}_e(90°)=\mathfrak{A}_n(90°)=2\pi(m_1m_3)^{\frac{1}{2}}E(1+E/E_g),$$
$$\mathfrak{A}_e(0°)=2\pi(m_2m_3)^{\frac{1}{2}}E(1+E/E_g),$$
$$\mathfrak{A}_n(0°)=2\pi(m_2m_3)^{\frac{1}{2}}E(1+E/E_g)^{\frac{1}{2}}F(\delta),$$

$$\left[\frac{\mathfrak{A}}{d\mathfrak{A}/dE}(0°)\right]_e=\left[\frac{\mathfrak{A}}{d\mathfrak{A}/dE}(90°)\right]_e$$
$$=\left[\frac{\mathfrak{A}}{d\mathfrak{A}/dE}(90°)\right]_n=E\frac{1+E/E_g}{1+2E/E_g},$$

$$\left[\frac{\mathfrak{A}}{d\mathfrak{A}/dE}(0°)\right]_n=E\left(1+\frac{E/E_g}{2(1+E/E_g)}-\frac{m_2'}{m_2}\frac{dF/d\delta}{F}\frac{E_g}{E}\right)^{-1},$$

where $\delta=(m_2'/m_2)(1+E/E_g)$ and $F(\delta)$, the result of evaluating elliptical integrals, and $dF/d\delta$ have the

following approximate values:

$$F(2)=1.06, \quad F'(2)=0.03, \quad F(3)=1.04, \quad F'(3)=0.01.$$

Hence for the case corresponding to bismuth, i.e., $E/E_g=\frac{1}{2}$ and $m_2=m_2'$, we have

$$\mathcal{A}_e(0°)/[2\pi E_g(m_2m_3)^{\frac{1}{2}}]=0.75,$$

$$\mathcal{A}_n(0°)/[2\pi E_g(m_2m_3)^{\frac{1}{2}}]=0.64,$$

$$\left[\frac{\mathcal{A}}{d\mathcal{A}/dE}(0°)\right]_e\Big/E_g=0.375,$$

$$\left[\frac{\mathcal{A}}{d\mathcal{A}/dE}(0°)\right]_n\Big/E_g=0.43.$$

Now Shoenberg obtains a value for A_{12}, the principal cross section through axes 1 and 2, by extrapolation using the ellipsoidal model. Thus, we see that if our special case of the non-ellipsoidal model holds, the actual area is only $0.64/0.75=85\%$ of his value. Hence we would expect a period $\approx 17\%$ higher than we would expect from the ellipsoidal model. Now magnetoresistance oscillations[14] for $\theta_0\approx 0$ (which do not disappear for $\theta_0=0$) are observed to give a period higher than what one might expect from the extrapolated ellipsoidal value and, qualitatively, the change in going to a non-ellipsoidal model is in the right direction to explain this. However, there is quantitative agreement between the magnetoresistance oscillation period and the period of Brandt's[15] very low temperature de Haas-van Alphen oscillations that are attributed to holes. Furthermore, there is no reason to believe that the holes should not dominate here since their cyclotron effective mass for this direction is smaller than that for the electrons. To find an unambiguous case of nonellipsoidal angular dependence, one would like to look at magnetoresistance oscillations without interference from the holes. The higher tellurium alloys of bismuth, since their hole bands are filled and since their E/E_g is higher, are ideal for such a study.

The mass corresponding to A_{23}, the principal cross section through axes 2 and 3, is so large that A_{23} cannot be inferred from de Haas-van Alphen measurements. Aubrey[10] determined it by multiplying $d\mathcal{A}/dE$ for this direction obtained in a cyclotron resonance experiment by Shoenberg's value of $\mathcal{A}(d\mathcal{A}/dE)^{-1}$. However, according to our analysis of the non-ellipsoidal theory, the correct $\mathcal{A}(d\mathcal{A}/dE)^{-1}$ for this direction is $0.430/0.375=1.15$ times as big as Shoenberg's. Hence the corresponding area should be 15% greater than that inferred by Aubrey.

TABLE IV. Variation of cross-sectional area with angle for $E/E_g=1$, $m_2/m_1=100$.

$\theta°$	0°	5°	15°	30°	45°	60°	90°
Ellipsoidal Cross section $[2\pi E_g(m_1m_3)^{\frac{1}{2}}]^{-1}$	20	15.1	7.25	3.94	2.82	2.30	2
Nonellipsoidal cross section $[2\pi E_g(m_1m_3)^{\frac{1}{2}}]^{-1}$	15.0	13.0	7.20	3.94	2.82	2.30	2

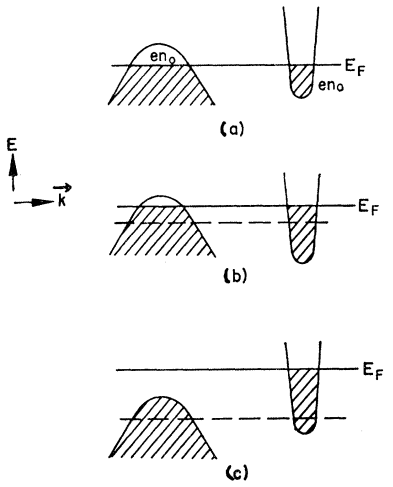

FIG. 9. Schematic diagram of the electron and hole bands, (a) in pure bismuth, (b) when enough electrons have been added to nearly fill the hole band, (c) when more than enough electrons to fill the hole band have been added.

C. Number of Ellipsoids

We will assume that the effect of adding a tellurium atom to bismuth is to add one electron to the Fermi sea and to affect negligibly the crystal potential. The assumption of the negligible disturbance of the crystal potential is reasonable since the addition of antimony, which is just to the left of tellurium in the periodic table but is not an electron donor or acceptor in bismuth, has negligible effect on the de Haas-van Alphen effect when added to bismuth in the concentration used here.[4] The assumption of the donation of one electron per tellurium atom will be justified in Sec. D.

The effect of adding electrons is shown in Fig. 9. In Fig. 9(a) we have pure bismuth with n_0 electrons and n_0 holes. Initially, some fraction of the electrons added goes into the hole band as shown in Fig. 9(b). Finally, after the hole band is filled, all of the electrons then added go into the electron band as shown in Fig. 9(c).

Now let N_a be the number of electrons added, V_0 be the phase space volume of conduction electrons in pure bismuth and V_a be the phase space volume after the addition of N_a electrons. Note that we can determine V_a/V_0 from the de Haas-van Alphen effect. Then if we plot N_aV_0/V_a vs N_a we get behavior as shown in Fig. 10. In curve (a) we have the situation for an infinite hole density of states. Here for $N_a<n_0$ all the electrons go into the hole band so that $V_0/V_a=1$ and we have a straight line of unit slope. After the hole band has been filled, which occurs for $N_a=n_0$ in curve (a), we have the following situation. The total number of electrons in the electron band $N_e=n_0$ (the initial number

[14] R. A. Connell and J. A. Marcus, Phys. Rev. **107**, 940 (1957).
[15] N. B. Brandt, A. E. Dubrouskaya, and S. A. Kytin, Soviet Phys. JETP **9**, 405 (1960).

TABLE V. Calculation of the number of electrons in bismuth.

	Tellurium added (10^{-3} at. %)	Electrons added N_a (10^{17} cm^{-3})	Scale factor s	Ellipsoidal $N_aV_0/V_a = N_as^{-\frac{3}{2}}$ (10^{17} cm^{-3})	E/E_g	Nonellipsoidal N_aV_0/V_a (10^{17} cm^{-3})
Present work	2.1±0.5	5.9±1.2	1.21	4.4±1.0	0.57	4.7±1.0
	3.8±0.5	10.7±1.2	1.55	5.5±0.6	0.67	5.9±0.6
	5.5±1.5	15.4±4.2	2.33	4.3±1.2	0.89	4.8±1.3
	13.4±0.7	37.6±2	4.0	4.7±0.3	1.27	5.7±0.4
Shoenberg and Uddin	1.8	5.1	1.3	3.4	0.60	3.5
	3.0	8.4	1.5	4.5	0.66	4.7
	4.5	12.6	1.8	5.3	0.74	5.7
	8.9	25	2.6	5.9	0.97	6.6

in pure bismuth)$+N_a$ (the total number added)$-n_0$ (those added which went to fill the hole band)$=N_a$. Now since $N_e=2V_a/h^3$ and $n_0=2V_0/h^3$ and since $N_e=N_a$, we have $N_aV_0/V_a=N_e\times 2h^3n_0/2h^3n_e=n_0$. Hence we see that after the hole band has been filled our curve has zero slope and a value n_0. The situation for a finite hole density of states is shown by curve b). Here the initial slope is less, and N_a is larger before the limiting value n_0 is reached.

Table V shows N_aV_0/V_a for various N_a using our data and, for reference, the data of Shoenberg and Uddin.[4] We have computed N_aV_0/V_a for two cases. The first, shown in column 4 is using the ellipsoidal parabolic model. Here if s is the ratio of the extremal cross section of the Fermi surface for any given angle in an alloy to that in bismuth, then $s^{\frac{3}{2}}$ is the corresponding phase space volume ratio. In the second case E/E_g is calculated for the various alloys using $E_{Bi}/E_g=0.49$ and $A_i=\beta_i=0$ in Cohen's theory. Here the relation

$$\frac{E}{E_g}\left(1+\frac{E}{E_g}\right)\Big/\frac{E_{Bi}}{E_g}\left(1+\frac{E_{Bi}}{E_g}\right)=s$$

gives us E/E_g as shown in column 5. Then using the formula

$$V=\frac{8\pi}{3}(8m_1m_2m_3E_g^3)^{\frac{1}{2}}\left(\frac{E}{E_g}\right)^{\frac{3}{2}}\times\left\{1+\frac{E}{E_g}\left[\frac{4}{5}\lambda+\frac{1}{5}\left(1+\frac{m_2'}{m_2}\right)\right]\right\} \quad (15)$$

for the volume we compute the column ratio for the case $m_2=m_2'$ and $\lambda=1$. The final result is shown in column 6.

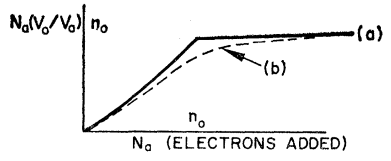

FIG. 10. Plot showing the behavior of the quantity N_0V_0/V_a versus N_a, (a) for the case of an infinite hole density of states, and (b) for a finite hole density of states.

From this we see that the use of our data and the nonellipsoidal model show the best consistency with the expected levelling off of N_aV_0/V_a for high N_a. From this we estimate that

$$n_0=(5.8\pm0.5)\times10^{17} \text{ electrons or holes/cc.}$$

In any case, all of the high N_a data give estimates of n_0 that lie in the range of $(5.4\pm1.2)\times10^{17}$ electrons or holes/cc.

To find the number of ellipsoids: we need to know the number of electrons/cc in a single ellipsoid in pure bismuth. For the case of $A_i=\beta_i=0$ we find that this number, which we shall call $\bar{n}$, is given by

$$\bar{n}=\frac{8}{3h^3\pi^{\frac{1}{2}}}(A_{12}A_{13}A_{23})^{\frac{1}{2}}\left\{\left(1+\frac{E/E_g}{1+E/E_g}\frac{m_2}{5m_2'}\right)F(\delta)\right\}. \quad (16)$$

Here A_{ij} are the cross sections of the "ellipsoid" made by planes passing through principal axes i and j. Using the results of Aubrey,[10] one can compute $\bar{n}=0.90\times10^{17}$ electrons/cc for a parabolic-ellipsoidal model. As we noted in Sec. B), if $A_i=\beta_i=0$ he overestimates A_{12} and underestimates A_{23} by about 15%. Hence his value of $(A_{12}A_{13}A_{23})^{\frac{1}{2}}$ is fortuitously correct. However, his use of the ellipsoidal-parabolic model is tantamount to having $\{\ \}=1$ in Eq. (16). For $E/E_g=\frac{1}{2}$ and $m_2=m_2'$ as we presume in bismuth, $\{\ \}=1.11$. Hence our estimate is $\bar{n}=1.00\times10^{17}$ electrons/cc "ellipsoid." Thus the multiplicity $r=n_0/\bar{n}$ is 5.8±0.5. It should be emphasized that all the formulas used are exact in the three "ellipsoid" case if $m_2=m_2'$. Hence we can say with confidence that there are not three but six "ellipsoids."

Now if we have six "ellipsoids," then either A_1, $\beta_1\neq0$ or A_2, A_3, β_2, $\beta_3\neq0$ by the symmetry arguments of Cohen.[2] But we find that if we assume $A_i=\beta_i=0$ that we calculate an r very close to 6 as well as the correct angular dependence for the de Haas-van Alphen effect. This indicates the likelihood that those A_i, β_i that do not vanish by symmetry are nevertheless small. However, a careful investigation of cases in the theory assuming large A_i and β_i would be necessary to show that our agreement is not accidental.

D. Density of States in Bismuth

Values given for the density of states in bismuth have varied rather widely. Kalinkina and Strelkov's[16] low-temperature specific heat work in very clean material gives 2.66×10^{-2}/ev atom after being corrected for nuclear quadrupole effects.[17,18] Phillips'[18] specific heat work in somewhat less pure material, again corrected for nuclear quadrupole effects, gives 0.89×10^{-2}/ev atom. Heine[19] obtains a value of 1.65×10^{-2}/ev atom from an interpretation of Shoenberg and Uddin's[4] experiments using the parabolic ellipsoidal model. We wish to construct a model of the hole band to rationalize this variation.

Our model must also accommodate the direct and reliable information about the holes in bismuth obtained from the cyclotron resonance experiments of Galt[20] and from the very low temperature de Haas-van Alphen measurements of Brandt.[21] Galt finds the shape of the hole Fermi surface an ellipsoid of revolution about the trigonal (3) axis with $m_1=m_2=0.068m_0$ and $m_3=0.92m_0$. Brandt finds the extremal cross sections for this surface of 6.75×10^{-42} g^2 cm^2/sec^2 for a plane perpendicular to the trigonal and 25.75×10^{-42} g^2/sec^2 for planes including the trigonal. The masses he determined are 30% lower than Galt's but he does not claim much accuracy for them. He gives the number of holes as $n_0=3.4\times10^{17}$/cc. Since the masses are relatively large, we may use the ellipsoidal model to determine a Fermi energy. Using Galt's masses and Brandt's areas, we find $T_F=135$°K.

Now if we make special assumptions or assume that certain experiments and their interpretations are either slightly or grossly in error, we can make many models. For example, if we reduce the number of holes per ellipsoid by 5% and increase the number of electrons per "ellipsoid" by 5% we can construct a 6 electron—2 light hole band model. We shall choose our model, however, so that it incorporates the cyclotron resonance and de Haas-van Alphen data directly and so that it can rationalize two prominent features of experiments on bismuth. These are the large, variable density of states and the relative insensitivity of the parameters of the light carriers to impurities.

Our model for the carriers in pure bismuth is as follows: six electron "ellipsoids" containing 6.0×10^{17} electrons/cc and with a Fermi temperature of 260°K as derived from the non-ellipsoidal model; one light hole ellipsoid with 3.4×10^{17} holes/cc and $T_F=135$°K; one heavy hole ellipsoid with the remaining 2.6×10^{17} holes/cc needed for charge neutrality and with $T_F=7$°K. The Fermi temperature of 7°K was chosen so as to fit Kalinkina and Strelkov's specific heat data to our model. We used Kalinkina and Strelkov's data as their material was considerably purer than that of Phillips.[17,18] With our model the electron density of states is 0.15×10^{-2}/ev atom and the light hole density of states is 0.16×10^{-2}/ev atom. Hence we need a contribution of 2.35×10^{-2}/ev atom from the heavy holes to get Kalinkina and Strelkov's value. For 2.6×10^{17} electrons/cc this requires $T_F=7$°K and, for a single ellipsoid, a density of states mass of $2.6m_0$. The latter decreases by the $\frac{2}{3}$ power of the multiplicity; multiplicities of 1, 2, 3, 6 and 12 being allowed by symmetry.

Now the model fulfills the requirements listed above. For assume we have 9 parts per million (ppm) donor impurities, which is not an unusual amount in bismuth when no special pains are taken for purification. Then the Fermi temperature will increase by $6\frac{1}{2}$°K. This will have a negligible effect on the light carrier properties, but it will almost fill the heavy carrier band and reduce the specific heat to Phillips value. Finally, it has been pointed out[13,17] that the presence of a large mass band near the Fermi surface seems necessary to explain the results of Jain.[13]

Following Heine,[19] we could also use the de Haas-van Alphen data from bismuth alloyed with acceptors to determine T_F for the heavy holes. Here we find some conflicting data in the work of Shoenberg and Uddin.[4] Their work shows, for example, that it takes ~150 ppm of Sn to reduce the electron extremal cross sections to $\frac{2}{3}$ of its value in pure Bi whereas it takes three times as much Pb for the same effect. If we assume that each Sn atom accepts one electron from the Fermi sea and apply the nonellipsoidal model, we find $T_F\sim12$° and a density of states of $\sim1.4\times10^{-2}$/ev atom for the heavy holes. If we apply the same assumptions to Pb, we find a T_F of $\sim5\frac{1}{2}$° and a density of states of $\sim2.9\times10^{-2}$/ev atom which is in better agreement with Kalinkina and Strelkov.[16] Now on theoretical grounds one would suppose that Sn or Pb should accept one electron per atom if they are acceptors. Since Shoenberg and Uddin[4] only claim order of magnitude accuracy for their Sn work and since their work on Pb has recently been well confirmed by Brandt and Razumenko,[22] the results for Pb would appear more reliable. However, Goetz and Focke[7] also find Sn~3 times as effective as Pb in changing the steady susceptibility. Because of this discrepancy, Kalinkina and Strelkov's[16] experiments would seem at present to give the most reliable estimate of T_F for the heavy holes. However, high-field galvanometric measurements in the alloys seem to be a potentially more powerful method. With them we can determine the change in T_F from their de Haas-van Alphen oscillations. Also, according to Mase,[23] we can determine

[16] I. N. Kalinkina and P. G. Strelkov, Soviet Phys. JETP **7**, 426 (1958).
[17] L. S. Lerner (to be published).
[18] N. E. Phillips, Phys. Rev. **118**, 644 (1960).
[19] V. Heine, Proc. Phys. Soc. (London) **A69**, 505, 513 (1956).
[20] J. K. Galt, W. A. Yager, F. R. Merritt, B. B. Celtin, and D. A. Brailsford, Phys. Rev. **114**, 1396 (1959).
[21] N. B. Brandt, Soviet Phys. JETP **11**, 975 (1960).
[22] N. B. Brandt and M. V. Razumenko, Soviet Phys. JETP **12**, 198 (1961).
[23] S. Mase (private communication).

the difference in hole and electron concentration directly from Hall and magnetoresistance measurements with H along the trigonal and with the current along another principal axis. This information will suffice to give us the density of states for our model. In any case, the acceptor alloying work to date indicates the need for a high density-of-states hole band.

Our model is also in good agreement with our data for alloy No. 1. For if we are to raise T_F by 40°K as in alloy No. 1, our model requires 2.6×10^{17} electron/cc to fill the heavy hole band completely, 1.5×10^{17} electrons/cc for the electron band, and 1.4×10^{17} for the light hole band. This gives a total of 5.5×10^{17} electrons/cc in good agreement with the $(5.9\pm1.2)\times10^{17}$ electrons/cc that we actually added.

Our data also disagree with some other models of the bismuth band structure. One of these is the 6 electron—2 light hole ellipsoid model mentioned before. This model is not necessarily in disagreement with the experiments showing a large density of states if we postulate a band with a heavy mass just below the Fermi surface in pure bismuth and further assume that these experiments were done in material with sufficient acceptor impurities. This model is also in rather good agreement with the anomalous skin effect work of Smith[24] although this does not necessarily mean that his work disagrees with our model. However, presuming that we started with pure material, this model requires 4.4×10^{17} electrons/cc to raise T_F by 40°, 1.6×10^{17} being for the electron band and 2.8×10^{17} for the hole band. This is considerably less than the $(5.9\pm1.2)\times10^{17}$ electrons/cc actually found necessary.

Another model our data for alloy No. 1 argues against is a 3 electron "ellipsoid"—1 light hole ellipsoid model. This model would be consistent with our results for alloys No. 2, No. 3, and No. 4 if we assumed on the average one-half an electron per tellurium donor atom. Now Goetz and Focke find that Se is only one-third as effective a donor as Te which we might interpret as showing that a donor does not necessarily contribute one electron to the Fermi sea. Again, however, this does not appear theoretically plausible, a boiling away of some of the rather volatile Se during crystal preparation seeming more likely. Now we can calculate that we require 2.2×10^{17} electrons/cc to raise T_F by 40°, 0.8×10^{17} for the electron band and 1.4×10^{17} for the hole band. This is considerably less than the $(3.0\pm0.6)\times10^{17}$ electrons/cc that we added assuming one-half an electron per Te atom. High field galvanomagnetic experiments in our higher Te alloys would be an ideal way to check this assumption as with them we can determine the number of electrons directly, holes being absent.

[24] G. E. Smith, Phys. Rev. **115**, 1561 (1959).

ACKNOWLEDGMENTS

The author wishes to express his gratitude to his sponsor, Professor A. W. Lawson, for continued support and encouragement, to Professor M. H. Cohen for many enlightening suggestions concerning the theoretical interpretation of the data, to Professor C. S. Barrett and Mr. L. S. Lerner for advice in sample preparation, and to Professor R. J. Donnelly for suggesting the method of suppressing the bubbling of liquid helium. He is also indebted to the Bell Telephone Laboratories and the National Science Foundation for graduate fellowship awards. The experimental work was supported by grants from the National Science Foundation, and by the Industrial Sponsors of the Institute for the Study of Metals.